Rotating black holes at future colliders: Greybody factors for brane fields

Daisuke Ida*
Department of Physics, Tokyo Institute of Technology, Tokyo 152-8551, Japan

Kin-ya Oda†
Physik Dept. T30e, TU München, James Franck Str., D-85748 Garching, Germany

Seong Chan Park‡
Korea Institute for Advanced Study (KIAS), Seoul 130-012, Korea
(Received 16 December 2002; published 31 March 2003)

We study theoretical aspects of rotating black hole production and evaporation in extra dimension scenarios with TeV scale gravity, within the mass range in which the higher dimensional Kerr solution provides a good description. We evaluate the production cross section of black holes, taking their angular momenta into account. We find that it becomes larger than the Schwarzschild radius squared, which is conventionally utilized in the literature, and our result nicely agrees with the recent numerical study by Yoshino and Nambu within a few percent error for the higher dimensional case. In the same approximation used to obtain the above result, we find that the production cross section becomes *larger* for a black hole with larger angular momentum. Second, we derive the generalized Teukolsky equation for spin 0, 1/2, and 1 brane fields in higher dimensional Kerr geometry and explicitly show that it is separable in any dimensions. For a five-dimensional (Randall-Sundrum) black hole, we obtain analytic formulas for the greybody factors in the low frequency expansion and we present the power spectra of the Hawking radiation as well as their angular dependence. The phenomenological implications of our results are briefly sketched.

DOI: 10.1103/PhysRevD.67.064025 PACS number(s): 04.70.Dy, 04.50.+h

I. INTRODUCTION

The fundamental gravitational scale can be lowered down to the TeV scale to remedy the hierarchy between the Planck and Higgs boson mass scales in the large extra dimension [Arkani-Hamed–Dimopoulos–Dvali (ADD)] scenario [1] (see also Ref. [2] for its stringy realization).[1] In the warped compactification (Randall-Sundrum) scenario, both of them scale together along the location in the warped extra dimension, leading again to the TeV fundamental scale at our visible brane [4]. When nature realizes such a TeV scale gravity scenario, it is predicted that black hole production will dominate over two-body scattering well above the fundamental scale, with a geometrical cross section of the order of the Schwarzschild radius squared [of the black hole mass equal to the center of mass (c.m.) energy of the scattering] [5]. Following the observation that black holes will mainly decay into the standard model fields on the brane rather than into the bulk modes [6], the collider signatures of black hole production and evaporation were studied comprehensively in Ref. [7] and independently in Ref. [8].[2] These two pioneering results have been applied in a lot of papers on the black hole phenomenology of the ultrahigh energy cosmic neutrino signature [10,11] and of collider signatures [12–14]. (In Ref. [15], it is claimed that the black hole production cross section would be exponentially suppressed rather than being geometrical; this was later answered by a semiclassical argument[3] [16] and by the correspondence principle applied to the production cross sections of black holes and strings [21].[4])

Black hole phenomenology opens up the fascinating possibility of *experimental investigation of quantum gravity* in the following sense. As is emphasized in Ref. [7], the black hole production hides all shorter distance processes than the Planck length scale behind the event horizon and infrared-ultraviolet duality emerges, i.e., the larger the c.m. energy becomes, the better is the semiclassical treatment [24] of the resultant black hole (since its Hawking temperature becomes lower). In string theory, where a nonperturbative definition is not yet established, this kind of situation (duality) often appears so that one picture is valid in one limit while the other is valid in the opposite limit (see, e.g., Ref. [25] for a review and also Refs. [26,21]). The region of true interest is the intermediate one at which both pictures break down and the nonperturbative formulation of quantum gravity (or string theory) becomes relevant. Given the status of the theoretical development, the experimental signature of quantum gravity

*Email address: d.ida@th.phys.titech.ac.jp
†Email address: odakin@ph.tum.de
‡Email address: spark@kias.re.kr

[1]When the number of extra dimensions is 2 (and hence their size is around the millimeter scale), the rather stringent cosmological constraint $M \gtrsim 100$ TeV is imposed [3].

[2]See also Ref. [9] for a study before this observation.

[3]The further claim that classical black hole formation in two-body scattering has been proved only with zero impact parameter [17] is answered in Refs. [18–20].

[4]We may observe a similar correspondence in the power of the exponential suppression of the hard scattering cross section [22], following the argument in Ref. [23].

in this intermediate region would be observed as a discrepancy with the semiclassical behavior in the black hole picture valid in the high energy limit. Therefore in order to investigate the quantum gravity effect, it is essential to predict this semiclassical behavior as precisely as possible. This is the main motivation of our work.

After the production phase (the ''balding'' phase), black holes are well described by the higher dimensional Kerr solution [27] if the mass of the produced black hole ($\simeq$ the c.m. energy of the collision) is large enough that we can neglect the brane tension at the horizon and also small enough that we can neglect the topology and curvature of the extra dimension(s) [7]. Within the CERN Large Hadron Collider (LHC) energy region, the former condition is satisfied (or marginal) and the latter is perfect in the ADD scenario [7,8] while the former is the same as in the ADD scenario and the latter is satisfied in the Randall-Sundrum scenario [when the horizon radius is smaller than the curvature length scale, which is one or two order(s) of magnitude larger than the Planck length scale[5]] [7,11]. Throughout this paper, we assume that both conditions are satisfied.

The black hole emits most of its quanta (and hence loses most of its mass and angular momentum) through Hawking radiation [24] when the above ''large enough'' (first) condition is satisfied and hence the few hot quanta emitted in the final ''Planck'' phase, which cannot be treated semiclassically, do not constitute the main part of the decay product [7]. (Remember that the smaller the black hole becomes, the hotter the Hawking radiation.) In most literature the ''spin-down'' phase of black hole evolution [7], in which the black hole sheds its angular momentum, is simply neglected and the Schwarzschild black hole is used from the start, relying on the four-dimensional result [32] that the half life for spin down is a few percent of the black hole lifetime.[6] To improve this ''Schwarzschild approximation,'' it is important to estimate the production cross section of black holes with finite angular momenta. In Ref. [33], the production cross section of rotating black holes is estimated from the quantum mechanical matrix element between the initial two-plane-wave state and the ''black hole state.'' In this paper, we take a more conservative approach based on the (classical) geometrical cross section,[7] in the spirit [16] that a classical description should be more or less valid for black hole production in order to avoid the Voloshin exponential suppression mentioned above.[8]

The Hawking radiation is determined for each mode by the greybody factor [24,31], i.e., the probability of absorption (by the black hole) of an incoming wave of the corresponding mode.[9] Unfortunately, the greybody factors have been calculated only for brane- and bulk-scalar modes with the Schwarzschild black hole at present [43]. In current black hole phenomenology, the Hawking radiation is either not considered (typically in the cosmic neutrino signature) or considered with the greybody factor in the geometrical optics limit.[10] To study the evaporation of a higher dimensional black hole and to make further progress in the phenomenology, it is a prerequisite to obtain the greybody factors of the brane fields (which are the main decay modes of the black hole as mentioned above).

In this paper, we obtain the brane field equations generalizing Teukolsky's method in four dimensions [38,40–42]. We show that they are separable into radial and angular parts. For the five-dimensional Kerr black hole, we find the analytic formulas of the greybody factors within the low frequency expansion.

In Sec. II, we present the geometrical production cross section of rotating black holes with finite angular momenta in the approximation neglecting the balding phase. Our result for the largest impact parameter $b_{\max}$ for black hole formation turns out to be in good agreement with the numerical result of Yoshino and Nambu [20]. Within the same approximation, we find that the (differential) cross section increases linearly with the angular momentum for a given black hole mass ($\simeq$ c.m. energy). We also estimate the production of the exploding black ring and find that it will possibly form when there are many extra dimensions. In Sec. III, we study the Hawking radiation from a rotating black hole. First we derive the brane field equations for spin 0, 1/2, and 1 brane fields from the induced metric on the brane in a higher dimensional Kerr black hole background and show that these equations are separable into radial and angular parts for any number of extra dimensions. Next we find the analytic expression for the greybody factors for brane fields for the rotating five-dimensional (Randall-Sundrum) black hole within the low frequency expansion. We present the power spectra as well as their angular dependence by applying these greybody factors. In Sec. IV, we present a summary and briefly comment on the phenomenological implications of our results.

II. PRODUCTION OF ROTATING BLACK HOLES

First we briefly review the properties of the rotating $(4+n)$-dimensional black hole [27]. Since we assume that the large enough condition (explained in the Introduction) is satisfied, the charges of the black hole can be neglected; there are at most a few coming from the initial two particles. In general, a higher dimensional black hole may have $\lfloor (n+3)/2 \rfloor$ angular momenta. When the black hole is produced in the collision of two particles on the brane, where the ini-

[5]References [28–30] considering mainly the application of the AdS/CFT correspondence also support this view.

[6]The spin-down phase accounts for about 25% of the mass loss in this four-dimensional case [32].

[7]See also Ref. [34] for an earlier heuristic attempt to estimate rotating black hole production.

[8]See Refs. [35,36] for the quantum argument, which also claim that Voloshin's suppression is not applicable.

[9]It was first calculated for a spin 0 field [37], then for spin 1 and 2 fields [38–42], and finally for a spin 1/2 field [31,32] for the four-dimensional Kerr black hole.

[10]See, e.g., Refs. [13,14] for consideration of the greybody factor in the geometrical optics limit for higher dimensional black holes.

tial state has only a single angular momentum (directed into the brane), it is sufficient to consider that the single angular momentum is nonzero [7]. (This implicitly assumes that the balding phase can be neglected, namely, that the "junk" emissions are negligible and do not change the $\lfloor (n+3)/2 \rfloor$ angular momenta during this phase.) In Boyer-Lindquist coordinates, the metric for a black hole with a single angular momentum takes the following form [27]:

$$g=\left(1-\frac{\mu r^{-n+1}}{\Sigma(r,\vartheta)}\right)dt^2-\sin^2\vartheta\left(r^2+a^2+a^2\sin^2\vartheta\frac{\mu r^{-n+1}}{\Sigma(r,\vartheta)}\right)\times d\varphi^2+2a\sin^2\vartheta\frac{\mu r^{-n+1}}{\Sigma(r,\vartheta)}dtd\varphi-\frac{\Sigma(r,\vartheta)}{\Delta(r)}dr^2-\Sigma(r,\vartheta)d\vartheta^2-r^2\cos^2\vartheta d\Omega^n, \quad (1)$$

where

$$\Sigma(r,\vartheta)=r^2+a^2\cos^2\vartheta,$$

$$\Delta(r)=r^2+a^2-\mu r^{-n+1}.$$

We can see that the horizon occurs when $\Delta(r)=0$, i.e., when $r=r_h$ with

$$r_h=\left[\frac{\mu}{1+a_*^2}\right]^{1/(n+1)}=(1+a_*^2)^{-1/(n+1)}r_S, \quad (2)$$

where $a_*=a/r_h$ and the Schwarzschild radius $r_S=\mu^{1/(n+1)}$ are introduced for later convenience. Note that there is only a single horizon when $n\geqslant 1$ (in contrast to the four-dimensional Kerr black hole, which has inner and outer horizons) and its radius is independent of the angular coordinates. We can obtain the total mass M and angular momentum J of the black hole from the metric (1):

$$M=\frac{(n+2)A_{n+2}}{16\pi G}\mu, \quad J=\frac{2}{n+2}Ma, \quad (3)$$

where $A_{n+2}=2\pi^{(n+3)/2}/\Gamma((n+3)/2)$ is the area of the unit sphere S^{n+2} and G is the $(4+n)$-dimensional Newton constant. Therefore we may consider μ and a (or r_h^{-1} and a_*) as the normalized mass and angular momentum parameters, respectively. We note that there is no upper bound on a when $n\geqslant 2$ nor on a_* when $n\geqslant 1$, in contrast to the four-dimensional case where both a and a_* are bounded from above. In this paper, we concentrate on the brane field equations and hence only the induced metric on the brane is relevant, where the last term in Eq. (1) vanishes and the angular variables ϑ and φ are redefined to take values $0\leqslant\vartheta\leqslant\pi$ and $0\leqslant\varphi<2\pi$. The explicit form is given in Eq. (A1).

A. Production cross section

We estimate the production cross section of rotating black holes within the classical picture. Let us consider a collision of two massless particles with finite impact parameter b and c.m. energy $\sqrt{s}=M_i$ so that each particle has energy $M_i/2$ in the c.m. frame. The initial angular momentum before collision is $J_i=bM_i/2$ (in the c.m. frame). Suppose that a black hole forms whenever the initial two particles (characterized by M_i and J_i) can be wrapped inside the event horizon of the black hole with mass $M=M_i$ and angular momentum $J=J_i$ (see Fig. 1 for a schematic picture), i.e., when

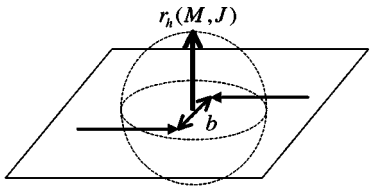

FIG. 1. Schematic picture for the condition of black hole formation.

$$b<2r_h(M,J)=2r_h(M_i,bM_i/2), \quad (4)$$

where $r_h(M,J)$ is defined through Eqs. (2) and (3). Since the right hand side is a monotonically decreasing function of b, there is a maximum value $b_{\max}$ which saturates the inequality (4):

$$b_{\max}(M)=2\left[1+\left(\frac{n+2}{2}\right)^2\right]^{-1/(n+1)}r_S(M), \quad (5)$$

where $r_S(M)$ is defined by $r_S(M)=\mu(M)^{1/(n+1)}$ and Eq. (3). When $b=b_{\max}$, the rotation parameter a_* takes the maximal value $(a_*)_{\max}=(n+2)/2$.

The formula (5) fits the numerical result for $b_{\max}$ with full consideration of general relativity by Yoshino and Nambu [20] within an accuracy of less than 1.5% for $n\geqslant 2$ and 6.5% for $n=1$ [although it just gives the Schwarzschild radius $b_{\max}=r_S(M)$ for $n=0$, which is 24% larger than the numerical result [18]] [see Table I, where R denotes $R=b_{\max}/r_S(M)$].

Our result is obtained in the approximation where we neglect all the effects of junk emissions in the balding phase and hence where the initial c.m. energy M_i and angular momentum J_i become directly the resultant black hole mass $M=M_i$ and angular momentum $J=J_i$.[11] The coincidence of our result with the numerical study [20] suggests that this approximation is actually viable for higher dimensional black hole formation at least unless b is very close to $b_{\max}$.[12]

[11]The authors of Ref. [20] found that the irreducible mass of the black hole is substantially reduced when b is close to $b_{\max}$ and suggested that the balding phase is not negligible when $b\sim b_{\max}$. However, the irreducible mass provides the lower bound on the final mass of the black hole; at this stage we cannot conclude how much junk energy and angular momentum are radiated at the balding phase.

[12]See Refs. [44–46] for estimation of the energy loss during the balding phase for the head-on collision ($b=0$) case obtained from gravitational radiation emitted during the infall of a particle into a four-dimensional black hole.

TABLE I. Comparison of analytical and numerical results for $b_{\max}/r_s$.

n	0	1	2	3	4	5	6	7
$R_{\text{numerical}}$ [20]	0.804	1.04	1.16	1.23	1.28	1.32	1.35	1.37
R_{analytic}	1.00	1.11	1.17	1.22	1.26	1.30	1.33	1.36

Once we neglect the balding phase and hence the junk emission, the initial impact parameter b directly leads to the resultant angular momentum of the black hole $J=bM/2$. Since the impact parameter $[b,b+db]$ contributes to the cross section $2\pi bdb$, this relation between b and J tells us the (differential) production cross section of a black hole with mass M and angular momentum in $[J,J+dJ]$

$$d\sigma(M,J)=\begin{cases} 8\pi JdJ/M^2 & (J<J_{\max}), \\ 0 & (J>J_{\max}), \end{cases} \tag{6}$$

where

$$J_{\max}=\frac{b_{\max}M}{2}=j_n\left(\frac{M}{M_P}\right)^{(n+2)/(n+1)} \tag{7}$$

with[13]

$$j_n=\left[\frac{2^n\pi^{(n-3)/2}\Gamma((n+3)/2)}{(n+2)[1+[(n+2)/2]^2]}\right]^{1/(n+1)},$$

$$M_P=\left(\frac{(2\pi)^n}{8\pi G}\right)^{1/(n+2)}. \tag{8}$$

The numerical values for j_n are summarized in Table II.

It is observed that the differential cross section (6) linearly increases with the angular momentum. We expect that this behavior is correct as the first approximation, so that the black holes tend to be produced with larger angular momenta. At the typical LHC energy $M/M_P=5$, the value of $J_{\max}$ is $J_{\max}=2.9,4.5,\ldots,10,12$ for $n=1,2,\ldots,6,7$, respectively. This means that the semiclassical treatment of the angular momentum becomes increasingly valid for large n.

Integrating the expression (6) simply gives

$$\sigma(M)=\pi b_{\max}{}^2=4\left[1+\left(\frac{n+2}{2}\right)^2\right]^{-2/(n+1)}\pi r_S(M)^2$$
$$=F\pi r_S(M)^2. \tag{9}$$

The factor F is summarized in Table III.

This result implies that, apart from the four-dimensional case, we would underestimate the production cross section of black holes if we did not take the angular momentum into account, and that it becomes more significant for higher dimensions. We point out that this effect has often been overlooked in the literature.

[13]See, e.g., Ref. [16] for different conventions for M_P.

TABLE II. Numerical values for j_n and k_n.

n	0	1	2	3	4	5	6	7
j_n	0.0398	0.256	0.531	0.815	1.09	1.37	1.63	1.88
k_n	0.0159	0.125	0.228	0.251	0.214	0.155	0.101	0.0603
k_n/j_n	0.399	0.489	0.429	0.308	0.195	0.114	0.0619	0.0320

B. Rotating black ring

In four dimensions, the topology of the event horizon must be homeomorphic to a two-sphere and there is uniqueness theorem for static or stationary black holes. On the other hand, a higher dimensional black hole can have various nontrivial topologies [47], and the uniqueness property of stationary black holes fails in five (and probably in higher) dimensions. A typical example in five dimensions has recently been given by Emparan and Reall [48]. They explicitly provided a solution of the five-dimensional vacuum Einstein equation, which represents the stationary rotating black ring (homeomorphic to $S^1\times S^2$). In this case, the centrifugal force prevents the black ring from collapsing. When the angular momentum is not large enough, the black ring will collapse to the Kerr black hole due to the gravitational attraction and some effective tension of the ring source. In fact, this five-dimensional black ring solution has the minimum possible value of the angular momentum given by

$$J_{\min}=k_{\text{BR}}\left(\frac{M}{M_P}\right)^{3/2}, \tag{10}$$

where $k_{\text{BR}}=0.282$. On the other hand, we have the upper bound for the angular momentum of the black holes produced by particle collisions:

$$J_{\max}=j_1\left(\frac{M}{M_P}\right)^{3/2}, \tag{11}$$

where $j_1=0.256$. Since these numerical values are of the same order, we cannot draw a conclusion about the possibility of black ring production at colliders.[14]

Here we consider the possibility of a higher dimensional black ring which is homeomorphic to $S^1\times S^n$. The corresponding Newtonian situation would be the system of a rotating massive circle. They are always unstable in higher dimensions; a circle with slow rotation collapses and one with rapid rotation explodes toward an infinitely large thin circle. In general relativity, we have no idea as to the validity of this picture due to the nonlinearity of the Einstein equation. We shall discuss in the following the possibility of black ring formation based on the Newtonian picture, assuming that the nonlinear effects of gravity do not change the qualitative features. For simplicity, we just consider the gravitational attraction and the centrifugal force of the massive circle and neglect the effect of tension. Let ℓ, M, and J

[14]Even if black rings are produced, they might be unstable due to the existence of $J_{\min}$ and the black string instability. D.I. is indebted to Roberto Emparan for this point.

TABLE III. Values of factor F in Eq. (9).

n	0	1	2	3	4	5	6	7
$F_{\text{numerical}}$ [20]	0.647	1.084	1.341	1.515	1.642	1.741	1.819	1.883
F_{analytic}	1.000	1.231	1.368	1.486	1.592	1.690	1.780	1.863

be the radius, the mass, and the angular momentum of the massive circle. Then we obtain $(3+n)$-dimensional effective theory with the Newton constant $G/2\pi\ell$ by integrating out along the S^1 direction. The Schwarzschild radius of the point mass in the effective theory is given by

$$r\sim\left[\frac{16\pi G}{(n+1)A_{n+1}}\frac{M}{2\pi l}\right]^{1/n}=\left[\frac{8GM}{(n+1)lA_{n+1}}\right]^{1/n}. \quad (12)$$

Thus we expect a black ring with S^1 radius ℓ and S^n radius r. In flat space picture, $\ell>r$ should hold for a black ring. This condition gives

$$\ell\gtrsim\ell_{\min}=\left[\frac{8GM}{(n+1)A_{n+1}}\right]^{1/(n+1)}. \quad (13)$$

On the other hand, the condition that the centrifugal force dominates against the gravitational attraction becomes

$$J\gtrsim 2^{-(n+3)/2}G^{1/2}\ell^{-(n-1)/2}M^{3/2}. \quad (14)$$

This combined with Eq. (13) gives the minimum value of the angular momentum for an exploding black ring:

$$J\gtrsim J_{\min}=k_n\left(\frac{M}{M_P}\right)^{(n+2)/(n+1)}, \quad (15)$$

where

$$k_n=2^{-(2n^2+3n+7)/2(n+1)}\pi^{(n+6)(n-1)/4(n+1)}\times\left[\frac{\Gamma((n+2)/2)}{n+1}\right]^{-(n-1)/2(n+1)}. \quad (16)$$

The numerical values for k_n are presented in Table II. This result shows that $J_{\min}$ for exploding black rings is one or two order(s) of magnitude smaller than $J_{\max}$ for the collision limit when n is large. Therefore we expect that exploding black rings can possibly be produced at colliders if there are many extra dimensions, although they will suffer from the black string instability when they become sufficiently large thin rings. In the rest of this paper, we do not follow the evolution of the exploding black ring nor consider the radiation from it, since this is still at the heuristic stage; we concentrate on the Hawking radiation from a higher dimensional Kerr black hole after the balding phase.

III. RADIATION FROM ROTATING BLACK HOLE

In this section, we study the Hawking radiation [24] from a higher dimensional Kerr black hole [27]. The Hawking radiation is thermal but not strictly blackbody due to the frequency dependent greybody factor Γ, which is identical to the probability of absorption (by the hole) of the corresponding mode [24,31]. The quantity $1-\Gamma$ for each mode can be computed from the solution (to the wave equation of that mode) having no outgoing fluxes at the horizon as the ratio of the incoming and outgoing flux at infinity.

It can be shown that a higher dimensional black hole radiates comparable amounts of energy into one brane mode and into one bulk mode (with the whole Kaluza-Klein tower summed up) [6]. Typically, the number of degrees of freedom is much larger for the brane mode than for the bulk mode, i.e., tens of the standard model degrees of freedom are living on the brane while there are only a few degrees of freedom of the graviton (and possibly other fields) in the bulk. Therefore a higher dimensional black hole radiates mainly on the brane [6]. For this reason, we concentrate on the greybody factors for the brane mode in this paper.[15]

A. Brane field equations

We derive the wave equations of the brane modes using the induced four-dimensional metric of the $(4+n)$-dimensional rotating black hole [27]. The wave equations can be understood as a generalization of the Teukolsky equation [38,40–42] to the higher dimensional Kerr geometry. The derivation is shown in the Appendix.

We present the brane field equations for a massless spin s field, which are obtained from the metric (1) with the standard decomposition

$$\Phi_s=R_s(r)S(\vartheta)e^{-i\omega t+im\varphi}, \quad (17)$$

utilizing the Newman-Penrose formalism [51]

$$\frac{1}{\sin\vartheta}\frac{d}{d\vartheta}\left(\sin\vartheta\frac{dS}{d\vartheta}\right)+[(s-a\omega\cos\vartheta)^2-(s\cot\vartheta+m\csc\vartheta)^2-s(s-1)+A]S=0, \quad (18)$$

$$\Delta^{-s}\frac{d}{dr}\left(\Delta^{s+1}\frac{dR}{dr}\right)+\left[\frac{K^2}{\Delta}+s\left(4i\omega r-i\frac{[2r+(n-1)\mu r^{-n}]K}{\Delta}\right)-n(n-1)\mu r^{-n-1}+2ma\omega-a^2\omega^2-A\right]R=0, \quad (19)$$

[15]We note that the bulk graviton emission may not be negligible for highly rotating black holes since the superradiant emission is more effective for higher spin fields [49,50].

where

$$K=(r^2+a^2)\omega-ma. \tag{20}$$

The solution of Eq. (18) is called spin-weighted spheroidal harmonics ${}_sS_{lm}$ (see, e.g., Refs. [41,52]) which reduces to spin-weighted spherical harmonics ${}_sY_{lm}$ (see, e.g., Ref. [53]) in the limit $a\omega \ll 1$,

$${}_sS_{lm}(a\omega;\vartheta,\varphi)={}_sY_{lm}(\vartheta,\varphi)+O(a\omega), \tag{21}$$

where[16]

$$\begin{aligned}{}_sY_{lm}(\vartheta,\varphi)=(-1)^m e^{im\varphi}\left[\frac{(l+m)!(l-m)!}{(l+s)!(l-s)!}\,\frac{2l+1}{4\pi}\right]^{1/2}\\ \times\left(\sin\frac{\vartheta}{2}\right)^{2l}\sum_j\binom{l-s}{j}\binom{l+s}{j+s-m}\\ \times(-1)^{l-j-s}\left(\cot\frac{\vartheta}{2}\right)^{2j+s-m},\end{aligned} \tag{22}$$

with the sum over j being understood in the range satisfying both $0\leqslant j\leqslant l-s$ and $0\leqslant j+s-m\leqslant l+s$. In this limit, the eigenvalue A becomes $A=A_0+O(a\omega)$ where $A_0=l(l+1)-s(s+1)$ is defined for later convenience.

We may easily check that the radial equation (19) reduces to the Teukolsky equation [38,40–42] when $n=0$ (hence $\mu=2GM$). The asymptotic solutions of Eq. (19) at the horizon and infinity are obtained in the same way as in four dimensions [42]:

$r\to\infty$		$r\to r_h$	
outgoing	ingoing	outgoing	ingoing
$e^{i\omega r_*}/r^{2s+1}$	$e^{-i\omega r_*}/r$	$e^{ikr_*}\Delta^{-s}$	e^{-ikr_*}

where

$$k=\omega-\frac{ma}{r_h^2+a^2}, \tag{24}$$

and r_* is defined by $r_*\to r$ for $r\to\infty$ and

$$\frac{dr_*}{dr}=\frac{r^2+a^2}{\Delta(r)}. \tag{25}$$

B. Hawking radiation and greybody factor

Since we have shown that the massless brane field equations are separable into radial and angular parts, we may write down the power spectrum of the Hawking radiation [24] for each massless brane mode as

$$\frac{dE_{s,l,m}}{dtd\omega d\varphi d\cos\vartheta}=\frac{1}{2\pi}\,\frac{{}_s\Gamma_{l,m}(r_h,a;\omega)}{e^{(\omega-m\Omega)/T}-(-1)^{2s}}\times|{}_sS_{lm}(a\omega;\vartheta,\varphi)|^2\omega, \tag{26}$$

where T and Ω are the Hawking temperature and the angular velocity at the horizon, respectively, given by

$$T=\frac{(n+1)+(n-1)a_*^2}{4\pi(1+a_*^2)r_h},\quad \Omega=\frac{a_*}{(1+a_*^2)r_h}, \tag{27}$$

and ${}_s\Gamma_{l,m}(r_h,a;\omega)$ is the greybody factor [24,31], which is identical to the absorption probability of the incoming wave of the corresponding mode. (In this paper we consider only the modes that can be treated as massless compared with the Hawking temperature T since the emissions from massive modes are Boltzmann suppressed; typically, the standard model fields can be treated as massless in the LHC energy range.) Integrating Eq. (26) by the angular variables, we obtain

$$\frac{dE_{s,l,m}}{dtd\omega}=\frac{1}{2\pi}\,\frac{{}_s\Gamma_{lm}}{e^{(\omega-m\Omega)/T}-(-1)^{2s}}\omega. \tag{28}$$

In the limit $a\omega\ll 1$ we can also write down the angular dependent power spectrum utilizing Eq. (21)

$$\frac{dE}{dtd\cos\vartheta d\omega}=\frac{1}{2\pi}\,\frac{{}_s\Gamma_{lm}}{e^{(\omega-m\Omega)/T}-(-1)^{2s}}\times\omega\left[\int_0^{2\pi}d\varphi|{}_sY_{lm}(\vartheta,\varphi)|^2\right], \tag{29}$$

where the integral in the square brackets can be done with Eq. (22); we summarize the results for the leading modes in Table IV.

Approximately, the time dependence of M and J can be determined by

$$-\frac{d}{dt}\begin{pmatrix}M\\ J\end{pmatrix}=\frac{1}{2\pi}\sum_{s,l,m}g_s\int_0^\infty d\omega\,\frac{{}_s\Gamma_{l,m}(r_h,a;\omega)}{e^{(\omega-m\Omega)/T}-(-1)^{2s}}\begin{pmatrix}\omega\\ m\end{pmatrix}, \tag{30}$$

where g_s is the number of "massless" degrees of freedom at temperature T, namely, the number of degrees of freedom whose masses are smaller than T, with spin s. (Typically $g_0=4$, $g_{1/2}=90$, and $g_1=24$ when $T>m_t,m_H$ and $g_0=0$, $g_{1/2}=78$, and $g_1=18$ when $m_b<T<m_W$ for the standard model fields.) Therefore, once we obtain the greybody factors, we have completely determined the Hawking radiation and the subsequent evolution of the black hole up to the

[16]The so-called Condon-Shortley phase $(-1)^m$ is inserted to reduce this to the standard definition of spherical harmonics when $s=0$: ${}_0Y_{lm}(\vartheta,\varphi)=Y_{lm}(\vartheta,\varphi)$.

TABLE IV. Results of integral in Eq. (29) for leading modes.

s	l	m	$\int_0^{2\pi} d\varphi \vert {}_sY_{lm}(\vartheta,\varphi)\vert^2$
0	0	0	1/2
0	1	1	$(3/4)\sin^2\vartheta$
0	1	0	$(3/2)\cos^2\vartheta$
0	1	-1	$(3/4)\sin^2\vartheta$
1/2	1/2	1/2	$\sin^2(\vartheta/2)$
1/2	1/2	$-1/2$	$\cos^2(\vartheta/2)$
1	1	1	$(3/8)(1-\cos\vartheta)^2$
1	1	0	$(3/4)\sin^2\vartheta$
1	1	-1	$(3/8)(1+\cos\vartheta)^2$

Planck phase, at which the semiclassical description using Hawking radiation breaks down and the few quanta radiated are not predictable.

In the high frequency limit, the absorption cross section for each mode $\sigma=(\pi/\omega^2)\Gamma$ is supposed to reach the geometrical optics limit (see, e.g., Refs. [13,14])

$$\sigma_{\text{g.o.}}=\pi\left(\frac{n+3}{2}\right)^{2/(n+1)}\frac{n+3}{n+1}r_H^2. \tag{31}$$

In all the phenomenological literature this limit has been applied when one calculates the Hawking radiation. [In Refs. [13,14] the phenomenological weighting factors 2/3 and 1/4 are used to multiply Eq. (31) for $s=1/2$ and $s=1$ fields, respectively, based on the result in four dimensions [31].]

C. Greybody factors for Randall-Sundrum black hole

To obtain the greybody factors from Eqs. (18) and (19) in general dimensions, we need a numerical calculation, which is beyond the scope of this paper and will be shown in Ref. [54]. In this paper we present an analytic expression for the greybody factors of brane fields for an $n=1$ Randall-Sundrum black hole within the low frequency expansion.[17] Here we outline our procedure. First we obtain the ''near horizon'' (NH) and ''far field'' (FF) solutions in the corresponding limits; then we match these two solutions at the ''overlapping region'' in which both limits are consistently satisfied; finally we impose the ''purely ingoing'' boundary condition at the near horizon side and then read the coefficients of ''outgoing'' and ''ingoing'' modes at the far field side; the ratio of these two coefficients can be translated into the absorption probability of the mode, which is nothing but the greybody factor itself.

First, for convenience, we define the dimensionless quantities

$$\xi=\frac{r-r_h}{r_h},\quad \tilde{\omega}=r_h\omega,\quad \tilde{Q}=\frac{\omega-m\Omega}{2\pi T}=(1+a_*^2)\tilde{\omega}-ma_*. \tag{32}$$

(Note that in the Schwarzschild limit $a_*\to 0$, $\tilde{Q}$ becomes $\tilde{Q}\to\tilde{\omega}$.) Then the radial equation (19) becomes

$$\xi^2(\xi+2)^2R_{,\xi\xi}+2(s+1)\xi(\xi+1)(\xi+2)R_{,\xi}+\tilde{V}R=0, \tag{33}$$

where

$$\tilde{V}=[\tilde{\omega}\xi(\xi+2)+\tilde{Q}]^2+2is\tilde{\omega}\xi(\xi+1)(\xi+2)-2is\tilde{Q}(\xi+1) -[A_0+O(a_*\tilde{\omega})]\xi(\xi+2). \tag{34}$$

In the near horizon limit $\tilde{\omega}\xi\ll 1$, the potential (34) becomes

$$\tilde{V}=\tilde{Q}^2-2is(\xi+1)\tilde{Q}-A_0\xi(\xi+2)+O(\tilde{\omega}\xi), \tag{35}$$

and the solution of Eq. (33) with the potential (35) is obtained with the hypergeometric function

$$\begin{aligned}R_{\text{NH}}=&C_1\left(\frac{\xi}{2}\right)^{-s-i\tilde{Q}/2}\left(1+\frac{\xi}{2}\right)^{-s+i\tilde{Q}/2}\\ &\times {}_2F_1\left(-l-s,l-s+1,1-s-i\tilde{Q};-\frac{\xi}{2}\right)\\ &+C_2\left(\frac{\xi}{2}\right)^{i\tilde{Q}/2}\left(1+\frac{\xi}{2}\right)^{-s+i\tilde{Q}/2}\\ &\times {}_2F_1\left(-l+i\tilde{Q},l+1+i\tilde{Q},1+s+i\tilde{Q};-\frac{\xi}{2}\right).\end{aligned} \tag{36}$$

To impose the ingoing boundary condition at the horizon (23), i.e.,

$$R\sim\xi^{-s}e^{-ikr_*},\quad k\frac{dr_*}{d\xi}\sim\frac{\tilde{Q}}{2\xi}, \tag{37}$$

we put $C_2=0$ and normalize $C_1=1$ without loss of generality, and then we obtain

$$\begin{aligned}R_{\text{NH}}=&\left(\frac{\xi}{2}\right)^{-s-i\tilde{Q}/2}\left(1+\frac{\xi}{2}\right)^{-s+i\tilde{Q}/2}\\ &\times {}_2F_1\left(-l-s,l-s+1,1-s-i\tilde{Q};-\frac{\xi}{2}\right).\end{aligned} \tag{38}$$

In the far field limit $\xi\gg 1+|\tilde{Q}|$, Eq. (33) becomes

$$0=R_{,\xi\xi}+\frac{2(s+1)}{\xi}R_{,\xi}+\left[\tilde{\omega}^2+\frac{2i\tilde{\omega}}{\xi}(s-2i\tilde{\omega}) -\frac{1}{\xi^2}[A_0+O(\tilde{\omega})]+O(\xi^{-3})\right]R, \tag{39}$$

and the solution is obtained via Kummer's confluent hypergeometric function

[17] See Ref. [55] for a study of the bulk scalar emission of a five-dimensional black hole.

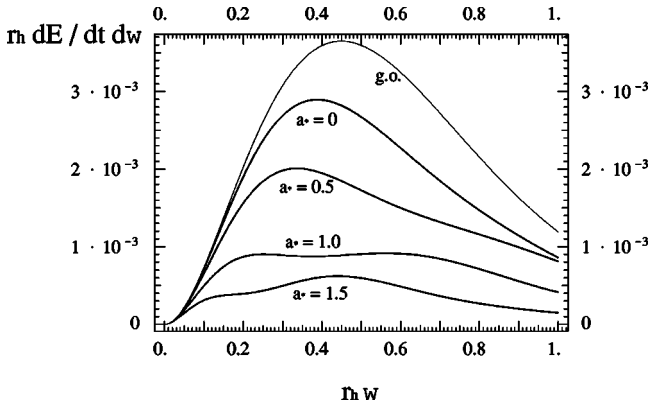

FIG. 2. Scalar ($s=0$) power spectrum $r_h dE/dtd\omega$ vs $\tilde{\omega}=r_h\omega$ in a linear-linear plot. The gray line corresponds the geometrical optics limit. The black lines are our results for $a_*=0$, 0.5, 1.0, and 1.5 from top to bottom. Note that our approximation is valid for $\tilde{\omega}<\min(1,a_*^{-1})$.

$$R_{\rm FF}=B_1 e^{-i\tilde{\omega}\xi}\left(\frac{\xi}{2}\right)^{l-s}{}_1F_1(l-s+1,2l+2;2i\tilde{\omega}\xi) + B_2 e^{-i\tilde{\omega}\xi}\left(\frac{\xi}{2}\right)^{-l-s-1}{}_1F_1(-l-s,-2l;2i\tilde{\omega}\xi), \tag{40}$$

where singularity from $2l$ being integer is regularized by the higher order terms in $\tilde{\omega}$.

Matching the NH and FF solutions (38) and (40) in the overlapping region $1+|\tilde{Q}|\ll\xi\ll 1/\tilde{\omega}$, we obtain

$$B_1=\frac{\Gamma(2l+1)\Gamma(1-s-i\tilde{Q})}{\Gamma(l-s+1)\Gamma(l+1-i\tilde{Q})},$$

$$B_2=\frac{\Gamma(-2l-1)\Gamma(1-s-i\tilde{Q})}{\Gamma(-l-s)\Gamma(-l-i\tilde{Q})}. \tag{41}$$

Then we extend the obtained FF solution toward the region $\xi\gg 1/\tilde{\omega}$,

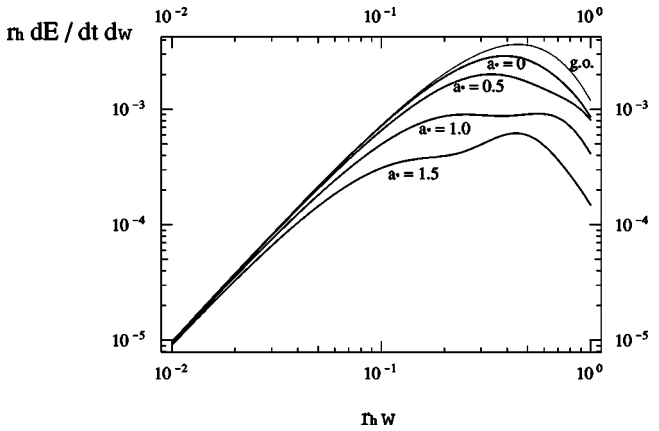

FIG. 3. Scalar ($s=0$) power spectrum $r_h dE/dtd\omega$ vs $r_h\omega$ in a log-log plot. See the caption of Fig. 2 for explanation.

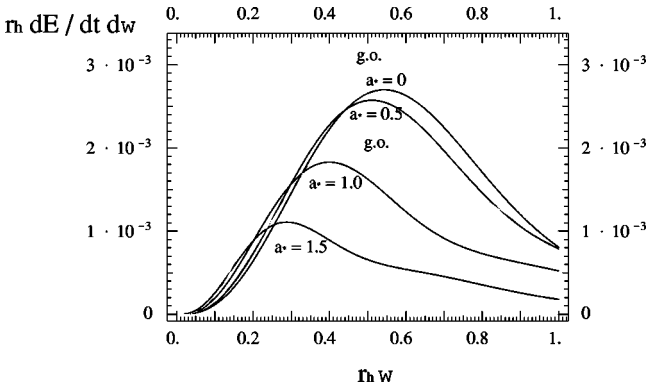

FIG. 4. Spinor ($s=1/2$) power spectrum $r_h dE/dtd\omega$ vs $\tilde{\omega}=r_h\omega$ in a linear-linear plot. The two gray lines (bottom and top) correspond to the geometrical optics limit with and without the phenomenological weighting factor 2/3, respectively. The black lines are our results for $a_*=0$, 0.5, 1.0, and 1.5, respectively, from right to left at the peak location. Note that our approximation is valid for $\tilde{\omega}<\min(1,a_*^{-1})$.

$$R_\infty=Y_{\rm in}e^{-i\tilde{\omega}\xi}\left(\frac{\xi}{2}\right)^{-1}+Y_{\rm out}e^{i\tilde{\omega}\xi}\left(\frac{\xi}{2}\right)^{-2s-1}, \tag{42}$$

where

$$Y_{\rm in}=\frac{\Gamma(2l+1)\Gamma(2l+2)}{\Gamma(l-s+1)\Gamma(l+s+1)}\frac{\Gamma(1-s-i\tilde{Q})}{\Gamma(l+1-i\tilde{Q})}(-4i\tilde{\omega})^{-l+s-1} + \frac{\Gamma(-2l)\Gamma(-2l-1)}{\Gamma(-l-s)\Gamma(-l+s)}\frac{\Gamma(1-s-i\tilde{Q})}{\Gamma(-l-i\tilde{Q})}(-4i\tilde{\omega})^{l+s},$$

$$Y_{\rm out}=\frac{\Gamma(2l+1)\Gamma(2l+2)}{[\Gamma(l-s+1)]^2}\frac{\Gamma(1-s-i\tilde{Q})}{\Gamma(l+1-i\tilde{Q})}(4i\tilde{\omega})^{-l-s-1} + \frac{\Gamma(-2l)\Gamma(-2l-1)}{[\Gamma(-l-s)]^2}\frac{\Gamma(1-s-i\tilde{Q})}{\Gamma(-l-i\tilde{Q})}(4i\tilde{\omega})^{l-s}. \tag{43}$$

Let us define R_{-s} as the solution of the equation obtained by a flip of the sign of s, i.e., $s\to -s$ from Eq. (19). When $\Delta_{,rr}=2$ as in $n=1$ (or as in the limit $r\gg r_H$ in $n\geqslant 2$), we may obtain the conserved current in the same way as in the four-dimensional case:

$$\mathcal{J}=\Delta(R_{-s}\partial_r R_s^*-R_s^*\partial_r R_{-s})+s\Delta_{,r}R_{-s}R_s^*, \tag{44}$$

which satisfies $\partial_r\mathcal{J}=0$. In the limit $r\gg r_H$,

$$R_s\sim Y_{\rm in}e^{-i\omega r}r^{-1}+Y_{\rm out}e^{i\omega r}r^{-2s-1},$$

$$R_{-s}\sim Z_{\rm in}e^{-i\omega r}r^{-1}+Z_{\rm out}e^{i\omega r}r^{2s-1}, \tag{45}$$

where $Z_{\rm in}=Y_{\rm in}|_{s\to -s}$ and $Z_{\rm out}=Y_{\rm out}|_{s\to -s}$, and $\mathcal{J}$ becomes

$$\mathcal{J}\sim 2i\omega(Z_{\rm in}Y_{\rm in}{}^*-Z_{\rm out}Y_{\rm out}{}^*). \tag{46}$$

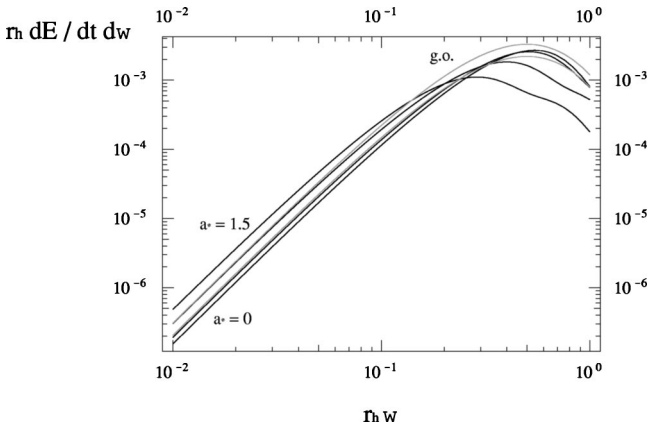

FIG. 5. Spinor ($s=1/2$) power spectrum $r_h dE/dtd\omega$ vs $r_h\omega$ in log-log plot. See the caption of Fig. 4 for explantion.

Therefore, we may calculate the greybody factor Γ (= the absorption probability) in the same way as Page's trick [31]

$$\Gamma = 1 - \left| \frac{Y_{\rm out} Z_{\rm out}}{Y_{\rm in} Z_{\rm in}} \right| = 1 - \left| \frac{1-C}{1+C} \right|^2, \tag{47}$$

where

$$C = \frac{(4i\tilde{\omega})^{2l+1}}{4} \left(\frac{(l+s)!(l-s)!}{(2l)!(2l+1)!} \right)^2 (-i\tilde{Q}-l)_{2l+1}, \tag{48}$$

with $(\alpha)_n = \Pi_{n'=1}^{n}(\alpha+n'-1)$ being the Pochhammer symbol.

For concreteness, we write down the explicit expansion of Eq. (47) up to $O(\tilde{\omega}^6)$ terms:

$$
\begin{aligned}
{}_0\Gamma_{0,0} &= 4\tilde{\omega}^2 - 8\tilde{\omega}^4 + O(\tilde{\omega}^6), \\
{}_0\Gamma_{1,m} &= \frac{4\tilde{Q}\tilde{\omega}^3}{9}(1+\tilde{Q}^2) + O(\tilde{\omega}^6), \\
{}_0\Gamma_{2,m} &= \frac{16\tilde{Q}\tilde{\omega}^5}{2025}\left(1 + \frac{5\tilde{Q}^2}{4} + \frac{\tilde{Q}^4}{4}\right) + O(\tilde{\omega}^{10}), \\
{}_{1/2}\Gamma_{1/2,m} &= \tilde{\omega}^2(1+4\tilde{Q}^2) - \frac{\tilde{\omega}^4}{2}(1+4\tilde{Q}^2)^2 + O(\tilde{\omega}^6), \\
{}_{1/2}\Gamma_{3/2,m} &= \frac{\tilde{\omega}^4}{36}\left(1 + \frac{40\tilde{Q}^2}{9} + \frac{16\tilde{Q}^4}{9}\right) + O(\tilde{\omega}^8), \\
{}_1\Gamma_{1,m} &= \frac{16\tilde{Q}\tilde{\omega}^3}{9}(1+\tilde{Q}^2) + O(\tilde{\omega}^6), \\
{}_1\Gamma_{2,m} &= \frac{4\tilde{Q}\tilde{\omega}^5}{225}\left(1 + \frac{5\tilde{Q}^2}{4} + \frac{\tilde{Q}^4}{4}\right) + O(\tilde{\omega}^{10}).
\end{aligned} \tag{49}
$$

Note that subleading terms in $\tilde{\omega}$ are already neglected when we obtain Eq. (47) and the terms from these contributions are not written nor included in Eqs. (47) and (49). We also note that the so-called *s*-wave dominance is maximally violated for spinor and vector fields since there are no $l=0$ modes for them.

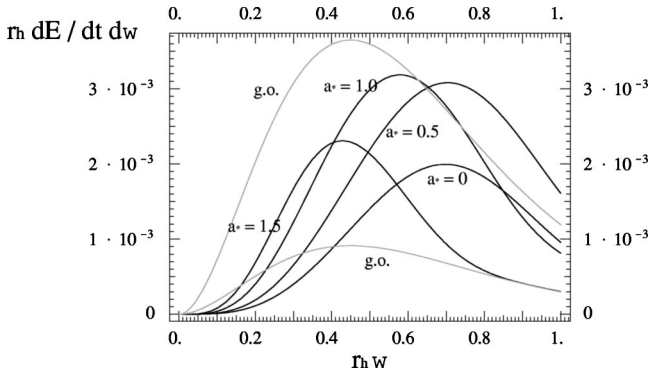

FIG. 6. Vector ($s=1$) power spectrum $r_h dE/dtd\omega$ vs $\tilde{\omega}=r_h\omega$ in a linear-linear plot. The two gray lines (bottom and top) correspond to the geometrical optics limit with and without the phenomenological weighting factor 1/4, respectively. The black lines are our results for $a_*=0$, 0.5, 1.0, and 1.5, respectively, from bottom to top at the left of the peaks. Note that our approximation is valid for $\tilde{\omega} < \min(1, a_*^{-1})$.

D. Radiation from Randall-Sundrum black hole

The greybody factor (47) is obtained from low frequency expansions. In four dimensions, it is known that the greybody factors in the low frequency expansion provide a smaller value for the right hand side of Eq. (30) than the one from a full numerical calculation [32]. Therefore in this paper we do not try to show the time evolution of the black hole nor the time-integrated result.

In Figs. 2–7, we show the power spectrum (28) for spin 0, 1/2, and 1 fields. The black lines are our results for $a_*=0$, 0.5, 1.0, and 1.5 utilizing the expression (47) with up to $l \leqslant 7$ modes, respectively, from bottom to top at the left of the peak (and from top to bottom at the right of the peak). Note that our approximation is valid for the region satisfying both $a_*\tilde{\omega}<1$ and $\tilde{\omega}<1$, typically at the left of the peak. The two gray lines (bottom and top) are the corresponding power

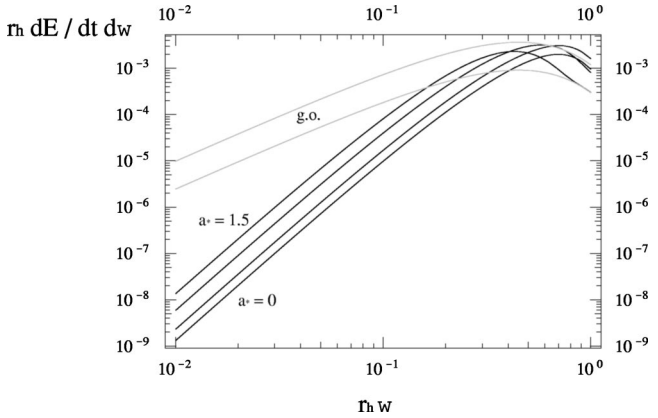

FIG. 7. Vector ($s=1$) power spectrum $r_h dE/dtd\omega$ vs $r_h\omega$ in a log-log plot. See the caption of Fig. 6 for explanation.

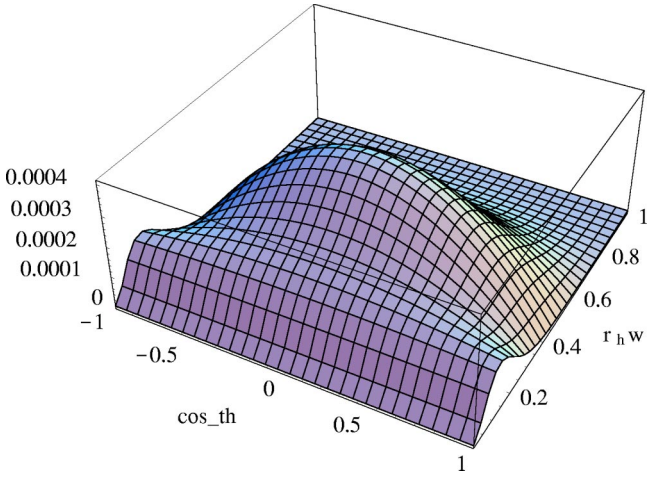

FIG. 8. Scalar ($s=0$) power spectrum $r_h dE/dtd\omega d\cos\vartheta$ vs $r_h\omega$ and $\cos\vartheta$ for $a_*=1.5$.

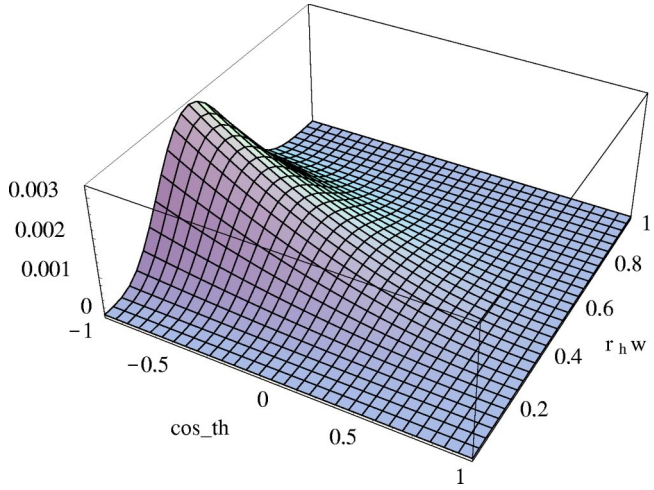

FIG. 10. Vector ($s=1$) power spectrum $r_h dE/dtd\omega d\cos\vartheta$ vs $r_h\omega$ and $\cos\vartheta$ for $a_*=1.5$.

spectra in the geometrical optics limit (31) with and without a phenomenological weighting factor, respectively (2/3 for spinors or 1/4 for vectors) [13,14].

In Figs. 8–10, we present the angular dependent power spectrum (29) for spin 0, 1/2, and 1 fields when $a_*=(a_*)_{\max}=1.5$. The modes are taken up to $l\leqslant 1$. We observe that there is a large angular dependence for spinors and vectors. Note that $\vartheta=0$ corresponds to the direction of the angular momentum of the black hole that is perpendicular to the beam axis. The angular dependence shown in Figs. 8–10 vanishes when we take the limit $a_*\to 0$.

IV. SUMMARY

We have studied theoretical aspects of rotating black hole production and evaporation.

For production, we present an estimation of the geometrical cross section up to unknown mass and angular momentum loss in the balding phase. Our result for the maximum impact parameter $b_{\max}$ is in good agreement with the numerical result by Yoshino and Nambu when the number of extra dimensions is $n\geqslant 1$ (i.e., within 6.5% when $n=1$ and 1.5% when $n\geqslant 2$), although our prediction is the same as the naive value in the Schwarzschild approximation $b_{\max}=r_S(M)$ when $n=0$, which is 24% larger than the numerical result. (Here we note that our refinement of the Schwarzschild approximation results in an enlargement of the production cross section, contrary to the previous claim in the literature.) Relying on this agreement, we obtain a (differential) cross section for a given mass and (an interval of) angular momentum, which increases linearly with the angular momentum up to the cutoff value $J_{\max}=b_{\max}M/2$. This result shows that black holes tend to be produced with large angular momenta. We also studied the possibility of black ring formation and find that a black ring would possibly form when there are many extra dimensions.

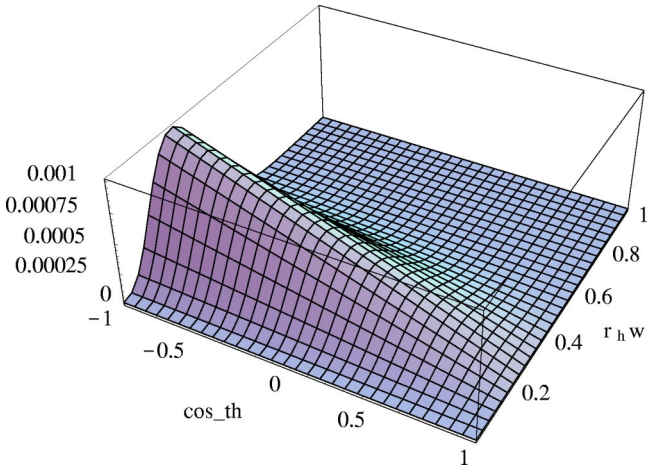

FIG. 9. Spinor ($s=1/2$) power spectrum $r_h dE/dtd\omega d\cos\vartheta$ vs $r_h\omega$ and $\cos\vartheta$ for $a_*=1.5$.

For evaporation, we first calculate the brane field equations for general spin and for an arbitrary number of extra dimensions. We show that the equations are separable into radial and angular parts like the four-dimensional Teukolsky equations. From these equations, we obtain the greybody factors for brane fields with general spin for a five-dimensional ($n=1$) Kerr black hole within the low frequency expansion. We present the resultant power spectrum which is substantially different from the one using the geometrical approximation utilized in the literature.

We address several phenomenological implications of our results. The production cross section of the black holes is larger than the one calculated from the Schwarzschild radius. A more precise determination of the radiation power is now available. We have shown that the black holes are produced with large angular momenta and that the resultant radiation will have strong angular dependence for the $s=1/2$ and $s=1$ modes which point perpendicular to the beam axis, while a very small angular dependence is expected for scalar modes. When we average over opposite helicity states, the up-down asymmetry with respect to the angular momentum axis shown in Fig. 9 disappears (although there still remains the angular dependence itself) [57,58]; we expect a similar result for the vector fields (which correspond to Fig. 10). A

more quantitative estimation will need the greybody factors for arbitrary frequency calculated numerically.

ACKNOWLEDGMENTS

We are grateful to Bob McElrath and Graham Kribs for helpful communications, and to Gungwon Kang and Manuel Drees for useful comments. D.I. would like to thank R. Emparan for discussions. D.I. was supported by JSPS Research, and this research was supported in part by the Grant-in-Aid for Scientific Research Fund (No. 6499). K.O. thanks to members of KIAS theory group for their hospitality during a visit and is grateful to the International Center for Elementary Particle Physics for financial support during the main period of this work. The work of K.O. is partly supported by the SFB375 of the Deutsche Forschungsgemeinschaft.

APPENDIX: SEPARABILITY OF BRANE FIELDS

The various field equations in the four-dimensional Kerr background are known to be separable. This results from the special feature of the four-dimensional Kerr metric, that is, the vacuum metric, which has a pair of degenerate principal null directions (Petrov type D). The four-dimensional metric considered in this paper is the induced metric of the totally geodesic probe brane in a higher dimensional Kerr field. Although this brane metric turns out to be of Petrov type D, it is not the vacuum metric itself. Nevertheless, it happens that the massless fields on the brane are separable, as shown below.

The induced metric on the three-brane in the $(4+n)$-dimensional Kerr metric (with a single nonzero angular momentum) is given in terms of the Boyer-Lindquist coordinate system by

$$g=\left(1-\frac{\mu}{\Sigma}r^{1-n}\right)dt^2+\frac{2a\mu}{\Sigma}r^{1-n}\sin^2\vartheta dt d\varphi-\sin^2\vartheta\left(r^2+a^2+\frac{\mu a^2\sin^2\vartheta}{\Sigma}r^{1-n}\right)d\varphi^2-\frac{\Sigma}{\Delta}dr^2-\Sigma d\vartheta^2, \tag{A1}$$

where

$$\Sigma=r^2+a^2\cos^2\vartheta,\quad \Delta=r^2+a^2-\mu r^{1-n}, \tag{A2}$$

and the parameters μ and a are equivalent to the total mass M and the angular momentum J

$$M=\frac{(n+2)A_{n+2}\mu}{16\pi G},\quad J=\frac{A_{n+2}\mu a}{8\pi G}, \tag{A3}$$

where $A_{n+2}=2\pi^{(n+3)/2}/\Gamma((n+3)/2)$ is the area of a unit $(n+2)$-sphere.

A direct calculation shows that the massless scalar field equation separates on this background geometry. If we set $\varphi=R(r)S(\vartheta)e^{-i\omega t+im\varphi}$, then $\nabla^2\varphi=0$ becomes

$$\frac{1}{\sin\vartheta}\frac{d}{d\vartheta}\left(\sin\vartheta\frac{dS}{d\vartheta}\right)+(a^2\omega^2\cos^2\vartheta-m^2\csc^2\vartheta+A)S=0, \tag{A4}$$

$$\frac{d}{dr}\left(\Delta\frac{dR}{dr}\right)+\left[\frac{K^2}{\Delta}+4i\omega r-i\frac{[2r+(n-1)\mu r^{-n}]K}{\Delta}-n(n-1)\mu r^{-n-1}+2ma\omega-a^2\omega^2-A\right]R=0, \tag{A5}$$

where $K=(r^2+a^2)\omega-am$. We note that the Hamilton-Jacobi and massive scalar field equations are also separable although we do not show them here; a test particle on the brane has an additional conserved quantity (Carter constant) in addition to the energy and the angular momentum.

To show the separability of higher spinor field equations, we work in the Newman-Penrose formalism [51].[18] We set the null tetrad as follows:

$$n_\mu=\delta^t_\mu-a\sin^2\vartheta\,\delta^\varphi_\mu-\frac{\Sigma}{\Delta}\delta^r_\mu,$$

$$n'_\mu=\frac{\Delta}{2\Sigma}(\delta^t_\mu-a\sin^2\vartheta\,\delta^\varphi_\mu)+\frac{1}{2}\delta^r_\mu,$$

$$m_\mu=\frac{i\sin\vartheta}{2^{1/2}(r+ia\cos\vartheta)}[a\,\delta^t_\mu-(r^2+a^2)\delta^\varphi_\mu]-\frac{r-ia\cos\vartheta}{2^{1/2}}\delta^\vartheta_\mu,$$

$$m'_\mu=\overline{m}_\mu, \tag{A6}$$

where the overbar denotes complex conjugation. These are subject to the normalization $n_\mu n'^\mu=-m_\mu m'^\mu=1$, $n_\mu n^\mu=n'_\mu n'^\mu=m_\mu m^\mu=n_\mu m^\mu=n'_\mu m^\mu=0$. An alternative description is given by the two-component spinor o^A,ι^A via the identification

$$(n^\mu,n'^\mu,m^\mu,m'^\mu)\leftrightarrow(o^A\overline{o^{A'}},\iota^A\overline{\iota^{A'}},o^A\overline{\iota^{A'}},\iota^A\overline{o^{A'}}), \tag{A7}$$

[18] See, e.g., Ref. [56] for a review of the Newman-Penrose formalism and spinor calculations. We follow the conventions of this reference.

with the symplectic structure $\epsilon^{AB}=o^A\iota^B-\iota^A o^B$, $\epsilon^{01}=\epsilon_{01}=1$. Each component of the spinor covariant derivative $\nabla_{AA'}$ is denoted by

$$(\nabla_{o\bar{o}},\nabla_{\iota\bar{\iota}},\nabla_{o\bar{\iota}},\nabla_{\iota\bar{o}})=(D,D',\delta,\delta'), \tag{A8}$$

and the spin coefficients are defined by

$$\begin{aligned} D(o,\iota)&=(\epsilon o-\kappa\iota,-\tau' o-\epsilon\iota),\\ D'(o,\iota)&=(-\epsilon' o-\tau\iota,-\kappa' o+\epsilon'\iota),\\ \delta(o,\iota)&=(\beta o-\sigma\iota,-\rho' o-\beta\iota),\\ \delta'(o,\iota)&=(-\beta' o-\rho\iota,-\sigma' o+\beta'\iota). \end{aligned} \tag{A9}$$

Then, all the nonzero spin-coefficients are[19]

$$\tau=-\frac{ia\sin\vartheta}{2^{1/2}\Sigma},\quad \rho=-\frac{1}{r-ia\cos\vartheta},\quad \beta=-\frac{\bar{\rho}\cot\vartheta}{2\sqrt{2}},$$

$$\tau'=-\frac{ia\rho^2\sin\vartheta}{\sqrt{2}},\quad \rho'=-\frac{\rho^2\bar{\rho}\Delta}{2},\quad \epsilon'=\rho'-\frac{\rho\bar{\rho}}{4}\Delta_{,r},$$

$$\beta'=\tau'+\bar{\beta}. \tag{A10}$$

Here, let us consider the Weyl equation ($s=1/2$) and the Maxwell equation ($s=1$) on this background brane metric.

We define the component of the Weyl spinor ψ_A simply by $\psi_0=\psi_A o^A$ and $\psi_1=\psi_A\iota^A$. Then, each component of the Weyl equation $\nabla^{AA'}\psi_A$ becomes explicitly

$$D\psi_1-\delta'\psi_0=(\beta'-\tau')\psi_0+(\rho-\epsilon)\psi_1, \tag{A11}$$

$$\delta\psi_1-D'\psi_0=(\epsilon'-\rho')\psi_0+(\tau-\beta)\psi_1. \tag{A12}$$

On the other hand, the Maxwell field is represented by the second-rank symmetric spinor ϕ_{AB}, and its components are denoted by $\phi_0=\phi_{AB}o^A o^B$, $\phi_1=\phi_{AB}o^A\iota^B$, and $\phi_2=\phi_{AB}\iota^A\iota^B$, respectively. Then, the source-free Maxwell equation $\nabla^{AA'}\phi_{AB}=0$ leads to

$$D\phi_1-\delta'\phi_0=(2\beta'-\tau')\phi_0+2\rho\phi_1-\kappa\phi_2, \tag{A13}$$

$$D\phi_2-\delta'\phi_1=\sigma'\phi_0-2\tau'\phi_1+(\rho-2\epsilon)\phi_2, \tag{A14}$$

$$D'\phi_0-\delta\phi_1=(\rho'-2\epsilon')\phi_0-2\tau\phi_1+\sigma\phi_2, \tag{A15}$$

$$D'\phi_1-\delta\phi_2=-\kappa'\phi_0+2\rho'\phi_1+(2\beta-\tau)\phi_2. \tag{A16}$$

The brane-induced metric turns out to be of Petrov type D, namely, the gravitational spinor Ψ_{ABCD} has only a non-zero component $\Psi_2=\Psi_{ABCD}o^A o^B\iota^C\iota^D$. In addition to this condition, when $\kappa=\sigma=\kappa'=\sigma'=0$ hold as in the present case, we have the identities for the differential operators

$$[D-(p+1)\epsilon+\bar{\epsilon}+q\rho-\bar{\rho}](\delta-p\beta+q\tau)-[\delta-(p+1)\beta+\bar{\beta}'-\bar{\tau}'+q\tau](D-p\epsilon+q\rho)=0, \tag{A17}$$

$$[D'-(p+1)\epsilon'+\bar{\epsilon}'+q\rho'-\bar{\rho}'](\delta'-p\beta'+q\tau')-[\delta'-(p+1)\beta'+\bar{\beta}-\bar{\tau}+q\tau'](D'-p\epsilon'+q\rho')=0, \tag{A18}$$

for any pair of numbers (p,q), where we have used the identities

$$\delta D-D\delta=(\bar{\tau}'-\bar{\beta}'+\beta)D+\kappa D'-(\bar{\rho}+\epsilon-\bar{\epsilon})\delta-\sigma\delta', \tag{A19}$$

$$\delta'D'-D'\delta'=\kappa' D+(\bar{\tau}-\bar{\beta}+\beta')D'-\sigma'\delta-(\bar{\rho}'+\epsilon'-\bar{\epsilon}')\delta'. \tag{A20}$$

Applying $(\delta+\bar{\beta}'-\bar{\tau}'-\tau)$ to Eq. (A11) and $(D+\bar{\epsilon}-\rho-\bar{\rho})$ to Eq. (A12), subtracting one from the other, and using Eq. (A17) for $(p,q)=(-1,-1)$, we obtain the decoupled equation for ψ_0:

$$\begin{aligned} &\left\{\left[\frac{(r^2+a^2)^2}{\Delta}-a^2\sin^2\vartheta\right]\frac{\partial^2}{\partial t^2}+2a\left(\frac{r^2+a^2}{\Delta}-1\right)\frac{\partial^2}{\partial t\partial\varphi}\right.\\ &\quad+\left(\frac{a^2}{\Delta}-\frac{1}{\sin^2\vartheta}\right)\frac{\partial^2}{\partial\varphi^2}+\left[2r-\frac{(r^2+a^2)\Delta_{,r}}{2\Delta}+ia\cos\vartheta\right]\frac{\partial}{\partial t}\\ &\quad+\left[-\frac{a\Delta_{,r}}{2\Delta}-\frac{i\cos\vartheta}{\sin^2\vartheta}\right]\frac{\partial}{\partial\varphi}-\Delta^{-1/2}\frac{\partial}{\partial r}\Delta^{3/2}\frac{\partial}{\partial r}\\ &\quad-\frac{1}{\sin\vartheta}\frac{\partial}{\partial\vartheta}\sin\vartheta\frac{\partial}{\partial\vartheta}+\frac{\cot^2\vartheta}{4}-\frac{1}{2}\\ &\quad\left.+n(n-1)\mu r^{-n-1}\right\}\psi_0=0. \end{aligned} \tag{A21}$$

If we set $\psi_0=R(r)S(\vartheta)e^{-i\omega t+im\varphi}$, then we obtain

$$\begin{aligned} &\frac{1}{\sin\vartheta}\frac{d}{d\vartheta}\left(\sin\vartheta\frac{dS}{d\vartheta}\right)+\left(a^2\omega^2\cos^2\vartheta-\frac{m^2}{\sin^2\vartheta}-a\omega\cos\vartheta\right.\\ &\quad\left.-\frac{m\cos\vartheta}{\sin^2\vartheta}-\frac{1}{4}\cot^2\vartheta+\frac{1}{2}+A\right)S=0, \end{aligned} \tag{A22}$$

$$\begin{aligned} &\Delta^{-1/2}\frac{d}{dr}\left(\Delta^{3/2}\frac{dR}{dr}\right)+\left[\left(\frac{K^2}{\Delta}+2i\omega r\right.\right.\\ &\quad\left.-\frac{i}{2}\frac{[2r+(n-1)\mu r^{-n}]K}{\Delta}\right)-n(n-1)\mu r^{-n-1}\\ &\quad\left.+2ma\omega-a^2\omega^2-A\right]R=0. \end{aligned} \tag{A23}$$

[19]Although we have defined the spin coefficients in spinor form, the tensor calculus would work better in actual computation. See Eqs. (4.5.28) in Ref. [56] for the equivalent tensorial definition for the spin coefficient.

For the Maxwell field, applying $(\delta-\beta+\overline{\beta}'-\overline{\tau}'-2\tau)$ to Eq. (A13) and $(D-\epsilon+\overline{\epsilon}-2\rho-\overline{\rho})$ to Eq. (A14), subtracting one from the other, and using Eq. (A17) for $(p,q)=(0,-2)$, we obtain

$$\left\{\left[\frac{(r^2+a^2)^2}{\Delta}-a^2\sin^2\vartheta\right]\frac{\partial^2}{\partial t^2}+\left[\frac{2a(r^2+a^2)}{\Delta}-2a\right]\frac{\partial^2}{\partial t\partial\varphi}+\left[\frac{a^2}{\Delta}-\frac{1}{\sin^2\vartheta}\right]\frac{\partial^2}{\partial\varphi^2}+\left[-\frac{\mu r^{-n}[(n+1)r^2+(n-1)a^2]}{\Delta}+2(r+ia\cos\vartheta)\right]\frac{\partial}{\partial t}+\left[-\frac{a[2r+(n-1)\mu r^{-n}]}{\Delta}-\frac{2i\cos\vartheta}{\sin^2\vartheta}\right]\frac{\partial}{\partial\varphi}-\frac{1}{\Delta}\frac{\partial}{\partial r}\Delta^2\frac{\partial}{\partial r}-\frac{1}{\sin\vartheta}\frac{\partial}{\partial\vartheta}\sin\vartheta\frac{\partial}{\partial\vartheta}+\cot^2\vartheta-1+n(n-1)\mu r^{-n-1}\right\}\varphi_0=0. \tag{A24}$$

Setting $\phi_0=R(r)S(\vartheta)e^{-i\omega t+im\varphi}$, then we have

$$\frac{1}{\sin\vartheta}\frac{d}{d\vartheta}\left(\sin\vartheta\frac{dS}{d\vartheta}\right)+\left(a^2\omega^2\cos^2\vartheta-\frac{m^2}{\sin^2\vartheta}-2a\omega\cos\vartheta-\frac{2m\cos\vartheta}{\sin^2\vartheta}-\cot^2\vartheta+1+A\right)S=0, \tag{A25}$$

$$\frac{1}{\Delta}\frac{d}{dr}\left(\Delta^2\frac{dR}{dr}\right)+\left[\frac{K^2}{\Delta}+4i\omega r-i\frac{[2r+(n-1)\mu r^{-n}]K}{\Delta}-n(n-1)\mu r^{-n-1}+2ma\omega-a^2\omega^2-A\right]R=0. \tag{A26}$$

In summary, the spin-s massless field equation becomes

$$\frac{1}{\sin\vartheta}\frac{d}{d\vartheta}\left(\sin\vartheta\frac{dS}{d\vartheta}\right)+[(s-a\omega\cos\vartheta)^2-(s\cot\vartheta+m\csc\vartheta)^2-s(s-1)+A]S=0 \tag{A27}$$

and

$$\Delta^{-s}\frac{d}{dr}\left(\Delta^{s+1}\frac{dR}{dr}\right)+\left[\frac{K^2}{\Delta}+s\left(4i\omega r-i\frac{[2r+(n-1)\mu r^{-n}]K}{\Delta}\right)-n(n-1)\mu r^{-n-1}+2ma\omega-a^2\omega^2-A\right]R=0. \tag{A28}$$

[1] N. Arkani-Hamed, S. Dimopoulos, and G. R. Dvali, Phys. Lett. B **429**, 263 (1998).

[2] I. Antoniadis, N. Arkani-Hamed, S. Dimopoulos, and G. R. Dvali, Phys. Lett. B **436**, 257 (1998).

[3] L. J. Hall and D. R. Smith, Phys. Rev. D **60**, 085008 (1999).

[4] L. Randall and R. Sundrum, Phys. Rev. Lett. **83**, 3370 (1999).

[5] T. Banks and W. Fischler, ''A model for high energy scattering in quantum gravity,'' hep-th/9906038.

[6] R. Emparan, G. T. Horowitz, and R. C. Myers, Phys. Rev. Lett. **85**, 499 (2000).

[7] S. B. Giddings and S. Thomas, Phys. Rev. D **65**, 056010 (2002).

[8] S. Dimopoulos and G. Landsberg, Phys. Rev. Lett. **87**, 161602 (2001).

[9] P. C. Argyres, S. Dimopoulos, and J. March-Russell, Phys. Lett. B **441**, 96 (1998).

[10] J. L. Feng and A. D. Shapere, Phys. Rev. Lett. **88**, 021303 (2002); L. Anchordoqui and H. Goldberg, Phys. Rev. D **65**, 047502 (2002); R. Emparan, M. Masip, and R. Rattazzi, *ibid.* **65**, 064023 (2002); Y. Uehara, Prog. Theor. Phys. **107**, 621 (2002); A. Ringwald and H. Tu, Phys. Lett. B **525**, 135 (2002); L. A. Anchordoqui, J. L. Feng, H. Goldberg, and A. D. Shapere, Phys. Rev. D **65**, 124027 (2002); M. Kowalski, A. Ringwald, and H. Tu, Phys. Lett. B **529**, 1 (2002); P. Jain, S. Kar, S. Panda, and J. P. Ralston, hep-ph/0201232; J. Alvarez-Muniz, J. L. Feng, F. Halzen, T. Han, and D. Hooper, Phys. Rev. D **65**, 124015 (2002); L. A. Anchordoqui, J. L. Feng, and H. Goldberg, Phys. Lett. B **535**, 302 (2002); S. I. Dutta, M. H. Reno, and I. Sarcevic, Phys. Rev. D **66**, 033002 (2002); H. Goldberg, A. D. Shapere, P. Jain, S. Kar, D. W. McKay, S. Panda, and J. P. Ralston, *ibid.* **66**, 065018 (2002); P. Gorham, J. Learned, and N. Lehtinen, astro-ph/0205170; L. A. Anchordoqui, J. L. Feng, H. Goldberg, and A. D. Shapere, Phys. Rev. D **66**, 103002 (2002).

[11] L. A. Anchordoqui, H. Goldberg, and A. D. Shapere, Phys. Rev. D **66**, 024033 (2002).

[12] K. Cheung, Phys. Rev. Lett. **88**, 221602 (2002); Phys. Rev. D **66**, 036007 (2002); A. Ringwald and H. Tu, Phys. Lett. B **525**, 135 (2002); S. Hofmann, M. Bleicher, L. Gerland, S. Hossenfelder, S. Schwabe, and H. Stocker, hep-ph/0111052; T. G. Rizzo, hep-ph/0111230; J. High Energy Phys. **02**, 011 (2002); G. Landsberg, Phys. Rev. Lett. **88**, 181801 (2002); M. Bleicher, S. Hofmann, S. Hossenfelder, and H. Stocker, Phys. Lett. B **548**, 73 (2002); Y. Uehara, hep-ph/0205122; hep-ph/0205199; K. Cheung and C. H. Chou, Phys. Rev. D **66**, 036008 (2002); A. Chamblin and G. C. Nayak, *ibid.* **66**, 091901(R) (2002).

[13] T. Han, G. D. Kribs, and B. McElrath, Phys. Rev. Lett. **90**, 031601 (2003).

[14] L. Anchordoqui and H. Goldberg, ''Black Hole Chromosphere at the LHC,'' hep-ph/0209337.

[15] M. B. Voloshin, Phys. Lett. B **518**, 137 (2001).

[16] S. B. Giddings, ''Black Hole Production in TeV-Scale Gravity, and the Future of High Energy Physics,'' hep-ph/0110127.

[17] M. B. Voloshin, Phys. Lett. B **524**, 376 (2002).

[18] D. M. Eardley and S. B. Giddings, Phys. Rev. D **66**, 044011 (2002).

[19] E. Kohlprath and G. Veneziano, J. High Energy Phys. **06**, 057 (2002).
[20] H. Yoshino and Y. Nambu, Phys. Rev. D **67**, 024009 (2003).
[21] S. Dimopoulos and R. Emparan, Phys. Lett. B **526**, 393 (2002).
[22] G.-w. Kang and K.-y. Oda (unpublished).
[23] K.-y. Oda and N. Okada, Phys. Rev. D **66**, 095005 (2002).
[24] S. W. Hawking, Commun. Math. Phys. **43**, 199 (1975).
[25] J. Polchinski, Rev. Mod. Phys. **68**, 1245 (1996).
[26] G. T. Horowitz and J. Polchinski, Phys. Rev. D **55**, 6189 (1997).
[27] R. C. Myers and M. J. Perry, Ann. Phys. (N.Y.) **172**, 304 (1986).
[28] S. B. Giddings, E. Katz, and L. Randall, J. High Energy Phys. **03**, 023 (2000).
[29] S. B. Giddings and E. Katz, J. Math. Phys. **42**, 3082 (2001).
[30] N. Arkani-Hamed, M. Porrati, and L. Randall, J. High Energy Phys. **08**, 017 (2001).
[31] D. N. Page, Phys. Rev. D **13**, 198 (1976).
[32] D. N. Page, Phys. Rev. D **14**, 3260 (1976).
[33] A. V. Kotwal and C. Hays, Phys. Rev. D **66**, 116005 (2002).
[34] S. C. Park and H. S. Song, ''Production of Spinning Black Holes at Colliders,'' hep-ph/0111069.
[35] S. N. Solodukhin, Phys. Lett. B **533**, 153 (2002).
[36] S. D. H. Hsu, ''Quantum production of black holes,'' hep-ph/0203154.
[37] A. A. Starobinsky, Sov. Phys. JETP **37**, 28 (1973).
[38] S. A. Teukolsky, Phys. Rev. Lett. **29**, 1114 (1972).
[39] A. A. Starobinsky and S. M. Churilov, Sov. Phys. JETP **38**, 1 (1974).
[40] S. A. Teukolsky, Astrophys. J. **185**, 649 (1973).
[41] W. H. Press and S. A. Teukolsky, Astrophys. J. **185**, 649 (1973).
[42] S. A. Teukolsky and W. H. Press, Astrophys. J. **193**, 443 (1974).
[43] P. Kanti and J. March-Russell, Phys. Rev. D **66**, 024023 (2002).
[44] V. Cardoso and J. P. S. Lemos, Phys. Lett. B **538**, 1 (2002).
[45] V. Cardoso and J. P. S. Lemos, ''The Radial Infall of a Highly Relativistic Point Particle into a Kerr Black Hole along the Symmetry Axis,'' gr-qc/0207009.
[46] V. Cardoso and J. P. S. Lemos, ''Gravitational Radiation from the Radial Infall of Highly Relativistic Point Particles into Kerr Black Holes,'' gr-qc/0211094.
[47] M.-l. Cai and G. J. Galloway, Class. Quantum Grav. **18**, 2707 (2001).
[48] R. Emparan and H. S. Reall, Phys. Rev. Lett. **88**, 101101 (2002).
[49] V. Frolov and D. Stojkovic, Phys. Rev. D **66**, 084002 (2002).
[50] V. Frolov and D. Stojkovic, Phys. Rev. Lett. **89**, 151302 (2002).
[51] E. Newman and R. Penrose, J. Math. Phys. **3**, 566 (1962).
[52] E. D. Fackerell and R. G. Crossman, J. Math. Phys. **18**, 1849 (1977).
[53] J. N. Goldberg, A. J. MacFarlane, E. T. Newman, F. Rohrlich, and E. C. G. Sudarshan, J. Math. Phys. **8**, 2155 (1967).
[54] D. Ida, K.-y. Oda, and S. C. Park (in progress).
[55] V. Frolov and D. Stojkovic, ''Quantum radiation from a 5-dimensional rotating black hole,'' gr-qc/0211055.
[56] R. Penrose and W. Rindler, *Spinors and Space-Time. 1. Two Spinor Calculus and Relativistic Fields*, Cambridge Monographs on Mathematical Physics (Cambridge University Press, Cambridge, England, 1984).
[57] A. Vilenkin, Phys. Rev. Lett. **41**, 1575 (1978).
[58] D. A. Leahy and W. G. Unruh, Phys. Rev. D **19**, 3509 (1979).